JOURNAL OF CHEMICAL INFORMATION AND MODELING

Article

pubs.acs.org/jcim

Identification of Novel Liver X Receptor Activators by Structure-Based Modeling

Susanne von Grafenstein,[†] Judit Mihaly-Bison,[∥] Gerhard Wolber,[§] Valery N. Bochkov,[∥] Klaus R. Liedl,[†] and Daniela Schuster*[,‡]

[†]Institute of General, Inorganic and Theoretical Chemistry/Theoretical Chemistry and Center for Molecular Biosciences Innsbruck (CMBI), University of Innsbruck, Innrain 80/82, A-6020 Innsbruck, Austria

[‡]Computer-Aided Molecular Design (CAMD) Group and CMBI, Institute of Pharmacy/Pharmaceutical Chemistry, University of Innsbruck, Innrain 80/82, A-6020 Innsbruck, Austria

[§]Institute of Pharmacy/Pharmaceutical Chemistry, Freie Universitaet Berlin, Koenigin Luise Strasse 2 + 4, D-14195 Berlin, Germany

[∥]Department of Vascular Biology and Thrombosis Research, Medical University of Vienna, Schwarzspanierstrasse 17, A-1090 Wien, Austria

Supporting Information

ABSTRACT: Liver X receptors (LXRs) are members of the nuclear receptor family. Activators of LXRs are of high pharmacological interest as LXRs regulate cholesterol, fatty acid, and carbohydrate metabolism as well as inflammatory processes. On the basis of different X-ray crystal structures, we established a virtual screening workflow for the identification of novel LXR modulators. A two-step screening concept to identify active compounds included 3D-pharmacophore filters and rescoring by shape alignment. Eighteen virtual hits were tested in vitro applying a reporter gene assay, where concentration-dependent activity was proven for four novel lead structures. The most active compound **10**, a 1,4-naphthochinone, has an estimated EC_{50} of around 5 μM.

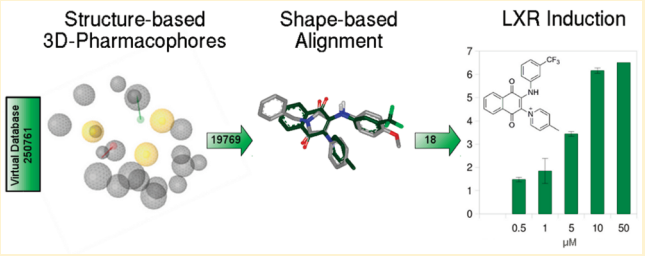

INTRODUCTION

Liver X receptors (LXRs) are members of the nuclear receptor family. The two subtypes α and β are classified in a homology-based nomenclature system as NR1H3 and NR1H2, respectively.[1] As lipid-activated nuclear receptors, they are composed of a highly conserved DNA binding domain (DBD) and a ligand binding domain (LBD), which can be targeted by endogenous ligands (oxidized cholesterol derivates),[2] as well as by synthetic ligands.[3] The regulatory impact of nuclear receptors on gene expression is linked with a conformational rearrangement of the LBD upon ligand binding, the dissociation of assembled corepressors or the recruitment of coactivators, and induced transcription effected by the DBD of the nuclear receptors. Enhanced transrepression of associated genes via LXR activation needs further studies, though already some insights in the complex inflammation related signaling pathways could be gained, as reviewed by Bensinger et al.[4,5]

The physiological impact of LXR is associated with the communicative interface of lipid metabolism and inflammation.[6,3] Therefore, the LXRs were identified as a promising drug target for indications such as hypercholesterolemia, atherosclerosis, and cardiovascular diseases.[7,4] Identification of first potent LXR agonists[8] and convenient results in vivo, such as promising experiments with atherosclerotic mice[9] motivated medicinal chemistry campaigns. Accelerated by insights into the molecular structure of the LXR LBD, various LXR-modulating scaffolds were identified and reviewed in refs 10 and 11. A striking setback on the road to the clinical application of LXR agonists is the increase of triglyceride levels in animal studies.[5] Strategies to overcome this side effect related with LXRα activation is the development of LXRβ-selective activators[12−14] or tissue-specific LXR modulators.[15] Detailed investigations revealed that the complex regulation processes in lipid metabolism might be considered as critical with regard to further potential side effects.[16] Nevertheless, potential uses as drug target remain attractive and the development of LXR modulators also including antagonists is an attractive research field.[17] Recently, LXR signaling was linked with acquired immune response,[18] proliferation control,[5] and antitumor response.[19] Furthermore, Alzheimer's disease[20,21] and diabetes[22] were added to the potential application fields of LXR modulators.

For the nuclear receptors LXRα and β 10 Brookhaven Protein Data Bank (PDB) entries were deposited from 2003 up to 2009 (Table 1).[23,24] The secondary structure of nuclear receptor ligand binding domains, dominated by 12 α-helices forming a mainly hydrophobic binding pocket, is highly

Received: February 17, 2012
Published: April 10, 2012

dx.doi.org/10.1021/ci300096c | J. Chem. Inf. Model. 2012, 52, 1391−1400

Table 1. Structural Data Available from PDB Deposits 2003−2009

PDB entry	ligand	resolution [Å]	subtype	gene source	crystal composition	refs
1p8d	**1**	2.80	β	human	homodimer, synthetic coactivator	39
1pq9	**2**[a]	2.10	β	human	homodimer	25
1pq6	**5**	2.40	β	human	homodimer	25
1pqc	**2**	2.80	β	human	homodimer	25
1upv	**2**	2.10	β	human	monomer	63
1upw	**2**	2.40	β	human	monomer	63
1uhl	**2**	2.90	α	human	dimer with RXRβ	64
2acl	**4**	2.80	α	mouse	dimer with RXRα	28
3fal	**3**	2.36	α	mouse	dimer with RXRα	27
3fc6	**6**	2.06	α	mouse	dimer with RXRα	26

[a]Ligand artifact from X-ray experiment.

conserved for the LXR structure of both subtypes. The PDB entry 1pq9 was excluded from this investigation as the ligand was destroyed during X-ray treatment of the crystal.[25] Full chains for the LBD are found in 1pq6, 1pqc, and 3fc6,[25,26] while the other crystal structures miss the 3D coordinates for several residues related to the flexibility of the protein. The PDB entries differ in resolution, cocrystallized proteins (monomers, homodimers, and physiological heterodimers with retinoid X receptor (RXR)), and the complexed ligands (Figure 1). Compound **1**, epoxycholesterol, is an endogenous LXR activator with weaker affinity than some published synthetic nonsteroid ligands. The hexaflouropropanol moiety in the sulfonamide T-0901317, compound **2**,[3] was optimized to compound **3** during structure guided design of the amide series by GSK.[27] Pharmacokinetic improvement efforts on compound **5**, GW3965,[8] led to the indol substituted compound **6**.[26] The maleimide structure of compound **4** represents a further scaffold and was identified by HTS.[28]

The published structural insights are a suitable basis for structure-based virtual screening (VS) strategies. The application of an approved computational high throughput screening (HTS) can be a faster and less expensive approach than classical experimental HTS in order to identify new scaffolds for LXR modulators. VS approaches have already been successfully applied on LXR. For instance, the identification of 2-aryl-*N*-acyl indole as LXR agonist, such as compound **6**, was guided by docking experiments.[29] The same working group published a successful docking campaign applying the program GLIDE to identify a further LXR modulating scaffold.[30] Two recent studies,[31,32] published during the preparation of this manuscript, also used 3D-pharmacophores to establish a VS protocol. Zhao et al. developed a ligand-based quantitative model for LXR agonists and validated their findings by docking.[32] The study of Ghemtio et al. has a similar methodological approach as the study we present here.[31] The authors compared a combination of 3D-pharmacophores and volume restrictions as prefilter for exhaustive docking.[33] However, our study goes a step further, as we included experimental testing of predicted virtual hits and thereby provide evidence for the model's validity.

RESULTS

Study Design. Crystallographic data from LXR LBD in complex with bioactive ligands, as found in the freely accessible PDB,[23,24] provided structural insights into the molecular interactions. In the concept of structure-based 3D-pharmacophores, the interacting features and their geometric relations are derived from the X-ray structures and translated into a

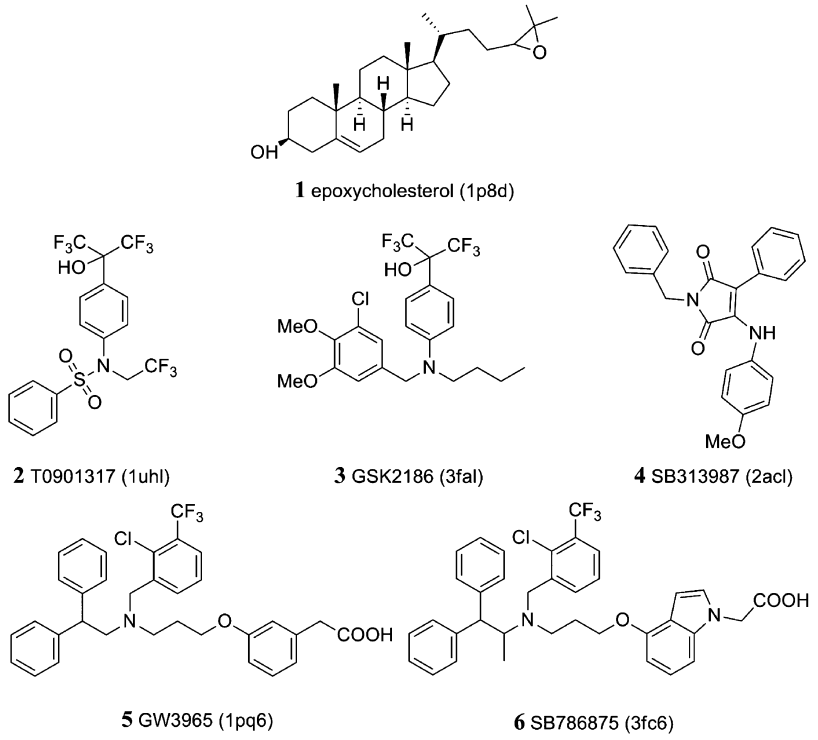

Figure 1. LXR modulators cocrystallized in PDB crystal structures.

dx.doi.org/10.1021/ci300096c | J. Chem. Inf. Model. 2012, 52, 1391−1400

pharmacophore model, which can be applied for screening of virtual compound databases reviewed in refs 34 and 35. In our study, we first included the 10 X-ray structures published up to 2009 covering LXR α as well as β, as the biological assay we applied is not suitable to distinguish subtype selectivity (Table 1). The pharmacophores, generated with LigandScout 2.3,[36] were manually modified and theoretically validated before seven pharmacophores derived from different PDB entries were selected for the VS. Applying multiple pharmacophores, we could cover different binding modes related with conformational changes in the binding pocket. The second step of VS was a reranking of the screening hit lists with the TanimotoCombo scoring function of ROCS, a method for fast alignment and comparison to the bioactive ligand conformation as query molecule.[37,38] The two-step in silico strategy was applied for screening of the National Cancer Institute (NCI) Database (250 761 compounds). Eighteen highly ranked compounds were selected from the hit list by aspects of availability, chemical diversity, and drug-like character for an in vitro transactivation assay, which verified LXR activation for four compounds. The work flow and key data are visualized in Figure 2.

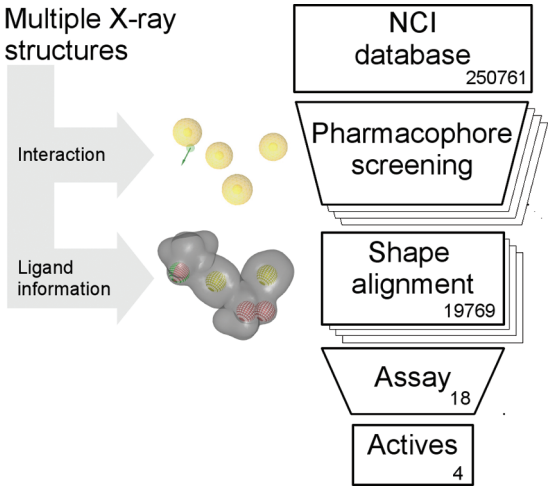

Figure 2. Workflow for finding novel LXR modulators.

LXR Ligand Binding Pocket. The binding sites of the LXRs are mainly hydrophobic and composed of two to three cavities and a tunnel directing to the solvent-exposed residues (C2) (Figure 3). In the C1 cavity, interaction with His435 (His421 in LXRα) is crucial and a hydrogen bond to this residue is supposed to stabilize the stacking of His435 to Trp457 (Trp443 in LXRα) in the C-terminal α-helix (known as helix 12), which favors the association of coactivators next to helix 12.[39] The epoxide oxygen of the endogenous ligand **1** forms this interaction as well as the synthetic compounds.[10] Although the hydrogen bond was described as critical, LXR modulators are known which do not establish a hydrogen bond to His435.[40] Small ligands, like compound **2**, fill the C1 and C2 region. The benzylsulfonate moiety extends a little into a wide tunnel, which is also present in the binding pocket with bound endogenous ligand. For comparison, larger molecules show another binding mode, where a third subpocket (C3) can open and accommodate branched hydrophobic substituents. This C3-cavity is formed by three phenylalanine residues. It is opened by an altered side chain conformation of Phe340. The

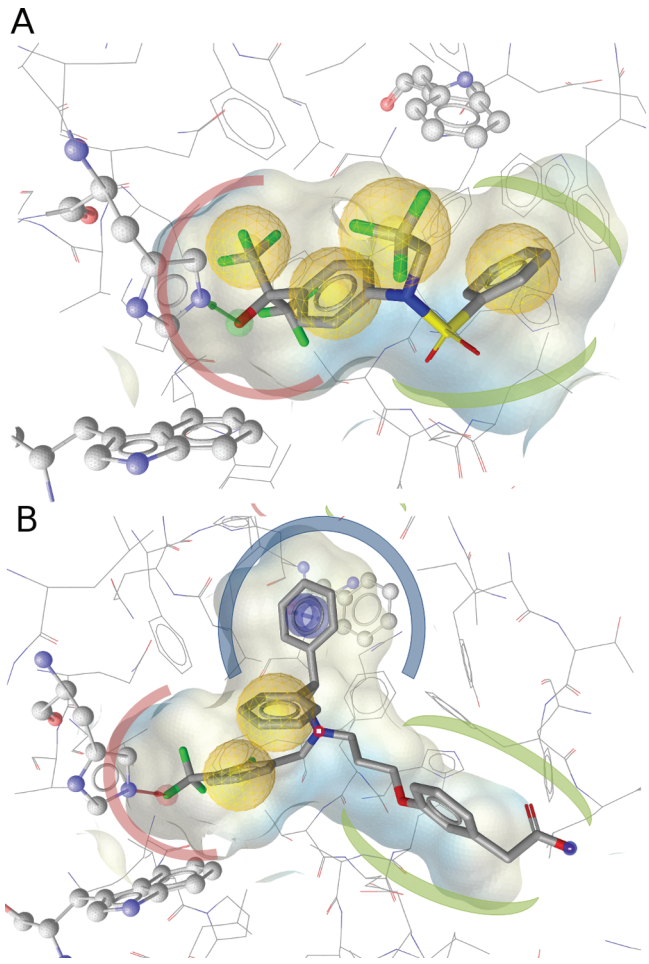

Figure 3. Binding pocket of compound **2** in 1pqc (A) and compound **5** in 1pq6 (B) with pharmacophore features of the models and highlighted cavity C1 (red), binding tunnel C2 (green), and subpocket C3 (blue); for the benefit of clear arrangement Xvols are hidden. His435, Trp443, and Phe340 are shown in ball and stick style. In part B, Phe340 changes its conformation and opens up the hydrophobic cavity C3 in order to accommodate the larger ligand compound **5**.

typical features of the binding pocket are reflected in the pharmacophore features.

Pharmacophore Models. The nine pharmacophore models generated based on PDB entries were composed of four to seven features describing ligand−receptor interactions and excluded volumes (Xvols) on protein atoms to line the binding pocket.[36] Initial pharmacophore generation was automated using the LigandScout algorithm and was followed by manual modification of the pharmacophore models. The optimization process aimed at improved enrichment factors, which describes the ratio of found active compounds versus hits from a decoy database (calculated according to the Experimental Section). To achieve a higher yield of active hits in the test set, selected features were deleted or modified. Further manipulations affected the spatial restriction for the pharmacophore models: While the standard approach placed single excluded volumes according to a residue-dependent algorithm (applied for the models 1p8d, 1pqc, 1uhl, 1upv, 1upw, 2acl, and 3fal), an alternative approach composed a coat of excluded volumes with a 0.8 Å tolerance on each heavy atom of the protein in the binding site (applied for the models 1pqc and 3fal). Composition of the nine pharmacophores is depicted

dx.doi.org/10.1021/ci300096c | J. Chem. Inf. Model. 2012, 52, 1391−1400

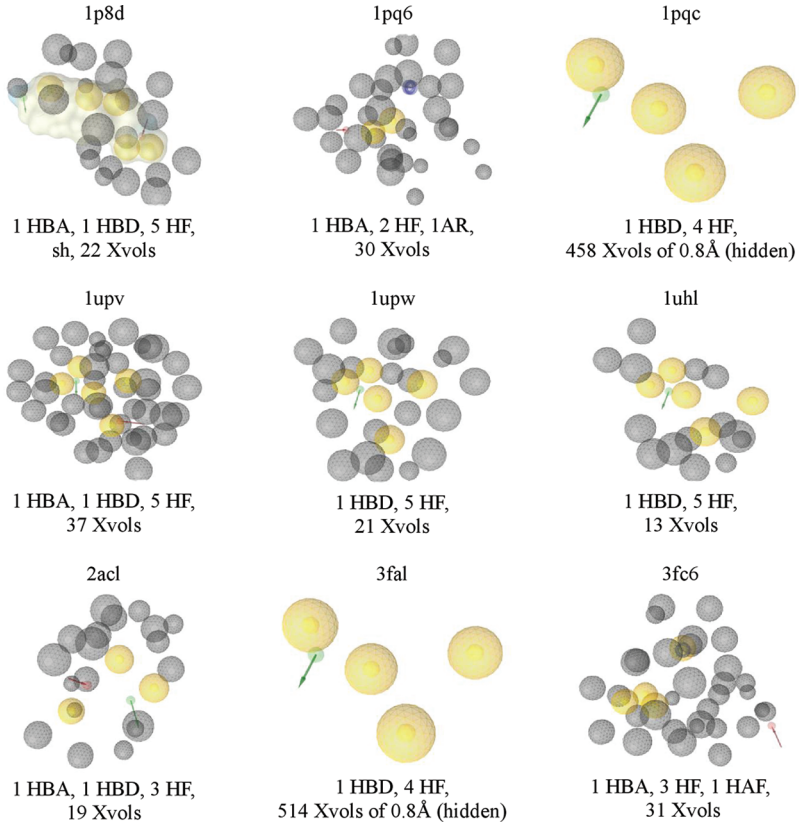

Figure 4. Pharmacophore models generated for LXR modulators. Chemical features are color-coded: hydrogen bond acceptor (HBA) red, hydrogen bond donor (HBD) green, hydrophobic (HF) yellow, aromatic ring feature (AR) blue, hydrophobic aromatic feature (HAF) blue and yellow, shape (sh), and exclusion volumes (Xvols) gray.

Table 2. Pharmacophore Characteristics

model code	1p8d[a]	1pq6	1pqc	1upv	1upw[a]	1uhl	2acl	3fal	3fc6	all	all w/o 1p8d 1upw
test set (41)	7	23	9	2	16	7	5	6	9	30	29
decoy set WDI (67050)	464	1699	2370	17	4338	1392	4916	1283	94	11318	9352
EF	24.9	22.4	6.3	176.6	6.2	8.4	1.7	7.8	146.6	4.4	5.2

[a]1p8d and 1upw were not used for subsequent virtual screening.

Table 3. Virtual and Biological Screening Results

model	1pq6	1pqc	1upv	1uhl	2acl	3fal	3fc6	combined
no. of hits from NCI (250 761)	4193	8078	56	2984	1875	5275	244	
no. of hits shape alignment	4116	7917	53	2906	1832	5183	243	19769
no. of selected compounds	7	7	2	9	5	6	1	18
no. of active compounds	1	2	1	4	2	1	0	4

in Figure 4, and their validation performance is summarized in Table 1. All pharmacophores besides model 3fc6 have hydrogen bond acceptors (HBA) which describe the interaction to His435. Central hydrophobic features (HF) in the binding site represent the hydrophobic character of the binding site. In model 3fal the additional C3 interaction is represented by a HF; in 3fc6, by a hydrophobic aromatic feature (HAF). In the model 1pq6, a more restrictive aromatic ring feature (AR) takes into account the orientation of the aromatic plane as further criterion for feature mapping as the ligand's phenyl moiety interacts via aromatic π-stacking to Phe340 (Figure 3). Pharmacophore model 2acl stands out with a very unfavorable enrichment factor. This is related to the distinct chemical scaffold of compound **6** and the fact that 1*H*-pyrrole-2,5-diones and related compounds were underrepresented in the test set.

The pharmacophores on PDB 1p8d and 1upw were excluded from the application phase of the screening system. With this study focusing on the identification of new nonsteroidal scaffolds, we decided to neglect the model 1p8d based on an endogenous ligand, which produced hit lists dominated by steroids during the validation screening. The enrichment factor of 6.2 for the model 1upw is typical for a crude filter, which could be useful for prescreening when followed by further filters for hit list reduction. In this study, the pharmacophore model 1upw is considered to be inappropriate as the pharmacophores are the only cutoff delimiter. Additionally, the 1upw model produced hits with high overlap to the model 1pqc during validation: only three test set hits of 1upw were

not matched by the model of 1pqc. Two of those test set compounds were covered by the models 1upv and 2acl. Therefore, exclusion of the model 1upw only had a minor effect on found actives from the test set, but resulted in a major reduction of the number of found decoys. The seven pharmacophore models used for subsequent screening matched 29 out of 41 active compounds in the test set and showed a combined enrichment factor of 5.2 in the validation screening.

Pharmacophore Screening. The parallel pharmacophore filtering of the NCI database resulted in seven virtual hit lists, one for each pharmacophore. The hit lists were composed of the compounds matching the pharmacophore model's chemical and geometrical restraints. The number of hits found by each model is displayed in Table 2. Mismatch between the NCI hit lists and the corresponding conformational hit lists is due to molecules failing the conformer generation algorithm of Openeye's Omega software, e.g. metal-containing compounds. The nonredundant, combined hit lists comprised 19 769 compounds corresponding to a filtering rate of 7.6%.

Shape Alignment. A subsequent ranking of the hit lists produced by pharmacophore screening was performed with shape based alignment applying Openeye's software ROCS. Bioactive conformations extracted from the crystal structures served as query molecules for alignment. A combination of shape overlap and chemical feature similarity between reference and the molecules from the hit lists (TanimotoCombo score) were applied for ranking. On the basis of this ranking, we selected 18 compounds for validation tests (Supporting Information, Table S1). The selection included highly ranked hits with conclusive alignment poses, low molecular weight (except one <500 g/mol), and chemical diversity. Three compounds contained a central sulfonamide and four compounds showed an aniline substructure, similar to the query compounds and other known LXR modulators. Nevertheless, the tested compounds also included new scaffolds, e.g., two acridine scaffolds and a 2,3-substituted naphthochinone.

LXR Reporter Assay. For 18 compounds the relative induction of the LXR-driven luciferase reporter gene was determined (Supporting Information, Table S2). Four compounds (**7**, **8**, **9**, and **10**, Figure 5, Table 4) showed a significant transactivation relative to the induction of ABCA1 transcription by the known LXR modulator **2**. Four compounds classified as active were reanalyzed at different compound concentrations (Figure 6). Compound **8** (NSC130822; 6-((benzyl((8-hydroxy-6-quinolinyl)methyl)amino)methyl)-8-quinolinol) and compound **10** (NSC618463; 2-(4-methyl-1Δ^5-pyridin-1-yl)-3-(3-(trifluoromethyl)anilino)naphthoquinone) induced ABCA1 transcription comparable to the known LXR activators **2** and **5**, but in higher concentrations. Compound **7** (NSC130101; 2-((diethylamino)methyl)-4-((4-methoxy-9-acridinyl)amino)phenol) and compound **9** (NSC131747; 4-(3-hydroxy-4-methoxybenzyl)-7-methoxy-8-isoquinolinol) even need concentrations of 50 μM to observe transactivation effects. Compound **9** showed the lowest absolute induction of ABCA1, what is in agreement with the results from relative induction experiments, where compound **9** at 25 μM showed 49.2% of induction compared to 1 μM of compound **2** (Supporting Information, Table S2).

DISCUSSION

The four identified LXR modulators were derived from a VS concept combining pharmacophore screening and rescoring with shape-based alignment.

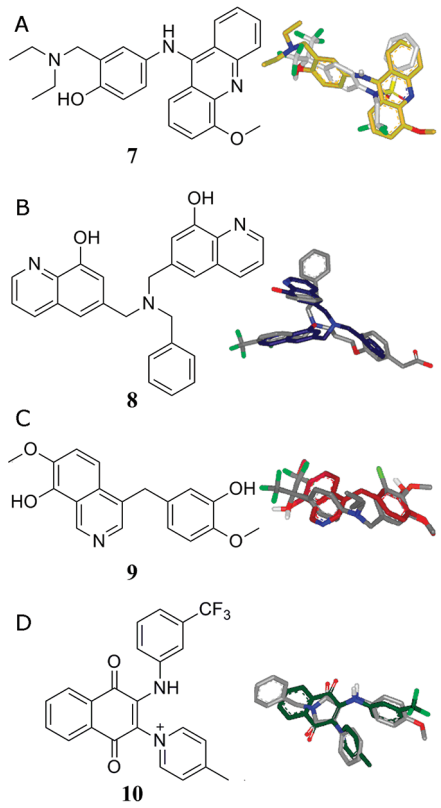

Figure 5. Newly identified LXR agonists and their shape alignment with the query compounds. (A) **7** with query compound **2** of 1upv. (B) **8** with query compound **5** of 1pq6. (C) **9** with query compound **3** of 3fal. (D) **10** with query compound **4** of 2acl.

Table 4. Newly Identified LXR Agonists

compound	hitlist, rank (shape-based)	rel induction ± SD[a] [%] 1 μM 25 μM
7	1pqc, 3471	13.6 ± 1.4*
	1upv, 5	90.9 ± 9.9*
	1uhl, 106	
	2acl, 601	
8	1pqc, 2837	44.9 ± 8.8
	1pq6, 42	76.7 ± 24.1
	3fal, 96	
9	3fal, 10	6.6 ± 2.7
		49.2 ± 10.5*
10	2acl, 55	53.4 ± 17.6
		109.7 ± 5.7*

[a]SD: standard deviation of three experiments.

With regard to the methodological aspects, this study joins a list of other screening approaches, which were already successful for other inflammatory targets and led to the identification of novel compounds targeting inflammation.[41−44] As far as we know, this is the first pharmacophore-based virtual screening published for the target LXR including biological confirmation. Nevertheless, the here presented screening concept for LXR is comparable to the structure based filtering strategies by Ghemtio et al.[31] The authors of the latter primarily focused on the comparative performance of the filters and finally proposed a consensus strategy for LXRβ. In contrast, our study is initially designed with a hierarchically condensation of two methods for VS and included LXRα and LXRβ.

dx.doi.org/10.1021/ci300096c | J. Chem. Inf. Model. 2012, 52, 1391−1400

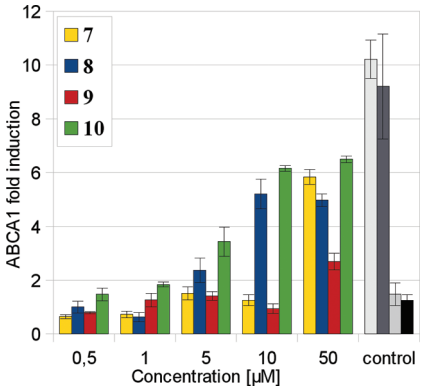

Figure 6. ABCA1 induction by compounds **7**, **8**, **9**, and **10** at different concentrations. The control includes ABCA1 induction of compound **2** at 1 μM (light gray) and compound **5** at 1 μM (anthracite) as well as unstimulated control with DMSO (gray) and without DMSO (black).

Additionally, our study integrated a biological testing for verification. Despite of these differences, we agree in many conceptual and methodological aspects. Similar to our approach, Ghemtio et al. applied parallel pharmacophores and shape filtering based on different crystal structures. The parallel conception is a convenient approach to overcome the challenges of a flexible drug target when multiple different crystal structures are available, as it is the case for LXR.[45,46]

Pharmacophore filtering and shape alignment, two virtual screening tools known for fast performance, are combined here. To show the synergy by the subsequent use of the two methods within this study, independent performance of both pharmacophore screening and shape alignment were analyzed retrospectively (Supporting Information Table S2 and S3). The four active compounds, **7**, **8**, **9**, and **10** are not ranked within the first 25% of the pharmacophore hit lists with the exception of compound **7** matching the model 1uhl with a good fit value. In respect, shape alignment alone without prefiltering by pharmacophores would not result in a top-ranking (top 500) for the active compounds. Top-ranked hits from both methods applied independently might still be active as no testing was performed to evaluate them as truly negative. However, we can state that neither pharmacophore nor shape alignment alone would have resulted in a selection of the four active compounds identified here. We conclude that the hierarchical combination of pharmacophore screening in a first step and shape alignment in a second one was crucial for the identification of the active LXR modulators.

A principle advantage of the parallel screening approach is that the modular conception allows for easily extending and adapting the approach to new insights. During manuscript preparation a further ligand-bound LXRβ structure was released in the PDB representing the binding mode of 4-(3-aryloxyaryl)-quinolines.[47] An additional pharmacophore model based on this new X-ray structure showed a hydrogen bond interaction with Leu330 (Supporting Information, Figure S2). This feature was not yet covered within the set of nine pharmacophore models. This hydrogen bond was suggested for LigandScout's automated pharmacophore generation in 3fc6 modeling but manually deleted in the model 3fc6 during model optimization. The new model 3kfc is characterized by a good hit rate in the test set (23/41) and partially complements the set of seven used pharmacophores by covering six additional test set compounds. Nevertheless, it shows also a high hit rate within the decoys, and because of this low restrictivity, we suggest not to include this new pharmacophore model 3kfc in further applications of the virtual screening approach.

Regarding the biological results, we could identify compounds **8** and **10** with EC_{50} around 5 μM and the weaker LXR activators **7** and **9**. Three of the active compounds show a molecular weight over 400 g/mol. The smallest compound (**9**, molecular weight 311.3 g/mol) being the weakest LXR activator in this study is a suitable candidate for lead optimization, as the small scaffold allows the addition of substituents targeting further interaction points within the spacious binding pocket. Compounds **7** and **8** showed more extended structures with four or more aromatic rings. Although the bulky acridine in compound **7** might be a steric challenge, **7** is matched by four pharmacophore models and the alignment within the structure 2acl complex predicts a convenient interaction pattern (Figure 7). Compound **8** showed no top-ranking in the alignment. Motivation to test compound **8** was the frequent occurrence of quinolin-8-ol substructures within the hit lists, and therefore, compound **8** with two quinolin-8-ol moieties and fair ranking within three hit lists was selected.

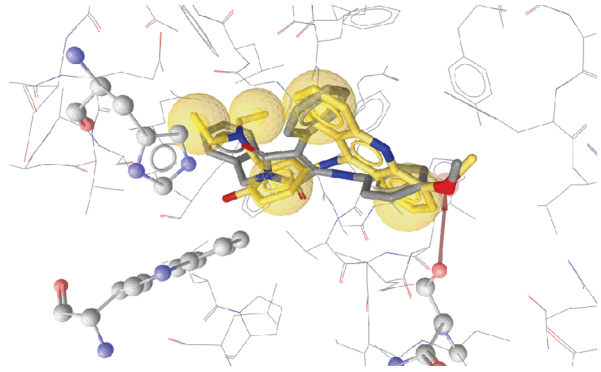

Figure 7. Alignment of compound **7** in the LXR crystal structure (PDB code 2acl). Five hydrophobic interactions and a hydrogen bond with Ser278 (LXRβ numbering) were identified with LigandScout. His435, Trp443, and Ser278 are shown in ball and stick style.

Compound **10** is of special interest, not only because of the highest activity found in this study but also for its interesting scaffold. The 2,3-substituted naphthochinone is different from known LXR modulators, and it is not surprising, that it was only found by the pharmacophore model 2acl, showing a distinct interaction pattern.[28] Alignment with the maleimide **4** showed perfect overlap for the aromatic substitute (Figure 5D), while the permanent charge of the pyridinyl substructure links to the basic function of other LXR activator classes, e.g. the tertiary amines as present in **3**, **5**, and **6**.

CONCLUSION

We presented a VS approach for the metabolic and immunological target LXR. Here the subsequent use of pharmacophore screening and shape alignment has been successful. The four novel compounds **7**, **8**, **9**, and **10** are identified as activators of LXR induced ABCA transactivation with low micromolar EC_{50} values and transactivation induction in levels comparable to known LXR activators. All four hits can serve as inspiration for lead optimization. Thus, the screening approach was evaluated positively and larger scale application is planned.

EXPERIMENTAL SECTION

Software Specification. The following software programs were used for this study: Inte:ligand's LigandScout 3.0 and Openeye's VIDA for visualization of 3D figures. Inte:ligand's LigandScout 2.3 for pharmacophore generation, Accelrys' Catalyst 4.11 for screening and calculation of multiconformer databases, Openeye's ROCS 2.4.2 for shape based alignment, and OMEGA 2.3.2 for calculation of multiconformer databases.

Compound Data Sets. Three compound databases were screened during this study. While a set of 41 LXR ligands (test set, Supporting Information, Figure S1) and a decoy set of drug-like compounds, the Derwent World Drug Index 2005 (WDI), were screened for pharmacophore validation, the third database was used for productive virtual screening (NCI database).

Forty-one ligands covering 12 scaffolds composed a validation data set, the so-called test set. The ligand structures and activity information were extracted from literature. We draw on a review by Bennett[10] and references therein, collecting LXR modulators published up to March 2007. Endogenous ligands and more recently published synthetic ligands completed our selection for the test set.[3,8,12−14,26,30,48−55] Compounds' 3D structures were prepared with CORINA 3.0[56] and the multiconformer database was calculated using Accelrys' Catalyst 4.11[57] (catConf settings: maximum number of conformers = 250/molecule, generation type = best quality, max. energy 20 kcal/mol above the calculated energy minimum). The WDI is a commercially available database with 67 050 drugs and biologically active compounds.[58] Here, we used this data set for selectivity check of the pharmacophores and considered these compounds as inactive decoys for the screening. The NCI database is the compound collection provided by the Developmental Therapeutic Program of the National Cancer Institute,[59] and a part of the compounds are provided for experimental research. The NCI data set, release 3, 2003 including 260 071 entries was downloaded and calculated as a multiconformational database using Catalyst for pharmacophore screening resulting in a 250 761 compound library (catconf settings: maximum number of conformers =100/molecule, generation type = fast). The hit lists as well as the NCI Database were calculated as multiconformational databases using OMEGA version 2.3.2 with the default setting to provide a format compatible with ROCS.

Pharmacophore Modeling, Screening, and Validation. The pharmacophores were generated applying LigandScout2.3 with default settings for the detection of protein−ligand interactions.[36] These primary pharmacophores were submitted to manual manipulation to exclude interactions with water molecules. The number of features for the primary pharmacophore models was reduced to make them more suitable for scaffold hopping during validation. VS was performed with the search engine of Accelrys' Catalyst 4.11 using the best flexible search option.[57]

To validate the models we screened the WDI as a collection of decoys and our test set including 41 LXR modulators. Calculating the enrichment factor (EF) helps to quantify the models discriminatory power:

$$\mathrm{EF} = (\mathrm{TP}/n)/(A/N)$$

where TP is the number of active LXR modulators matched by the model, n is the sum of LXR modulators and decoys matched by the model, A is the number of active LXR modulators within the test set, and N is the number of all compounds in the validation data sets.[60]

Shape Alignment. The command line application ROCS 2.4.2 performs automated alignment of investigated compounds to a query molecule optimizing the overlap of the shape, which is characterized by a sum of continuous Gaussian functions.[38] ROCS optimizes the shape overlap and produces a scoring function according to the Tanimoto equation,

$$\mathrm{Tanimoto}_{\mathrm{f,g}} = O_{\mathrm{f,g}}/(I_{\mathrm{f}} + I_{\mathrm{g}} - O_{\mathrm{f,g}})$$

where I terms are the self-volume overlaps for the query molecule f and a compared molecule g and the overlap $O_{\mathrm{f,g}}$, was maximized during alignment.

A further ROCS score is the ColorTanimoto, which calculates the overlap of the six chemical features (hydrogen-bond donors, hydrogen-bond acceptors, hydrophobes, anions, cations, and rings), defined with the ImplicitMillsDean force field.[61] The TanimotoCombo, which simply adds the two scores ShapeTanimoto and ColorTanimoto, was used for the ranking of the pharmacophore-based hit lists. It can take values between 0 and 2. We used the conformations of cocrystallized LXR activators from the PDB entries as query molecules for the alignment of the hit lists produced by the pharmacophores derived from the same PDB entry

LXR Reporter Assay. A bioluminescence assay using the luciferase reporter construct driven by *ABCA1* gene promoter was used to quantify the activity of potential LXR modulators. All experimental conditions were exactly as described by us recently,[62] except for overexpressing human LXRβ and using ABCA1 promoter-driven reporter. The induction relative to compound **2** (100%) was determined for all 18 compounds performing three repeats for each experiment at 1 and 25 μM concentration, respectively. Two experiments at 25 μM were not possible due to solubility problems. For four active compounds, additional dose-dependency experiments were performed at five concentrations, and these experiments were evaluated for EC_{50} estimations.

ASSOCIATED CONTENT

Supporting Information

Structures and transactivation assay results of the 18 tested compounds, the comparative analysis of independent pharmacophore and shape-based screening, the test set of compounds used for validation, and the pharmacophore modeling for 3kfc. This material is available free of charge via the Internet at http://pubs.acs.org.

AUTHOR INFORMATION

Corresponding Author

*E-mail: Daniela.Schuster@uibk.ac.at.

Notes

The authors declare no competing financial interest.

ACKNOWLEDGMENTS

This work was part of the national research network "Drugs from Nature Targeting Inflammation−DNTI" projects number S107 sponsored by the Austrian Science Fund FWF (subprojects S1072/S10711 and S10709/S10713). Test compounds were provided free of charge by the National Cancer Institute. We thank Dr. Rémy D. Hoffmann, Accelrys SARL Paris, for screening the Derwent WDI database and Patrick

Markt, Johannes Kirchmair, Stefan Noha, and Gudrun Spitzer for discussion on methodical issues as well as Judith Rollinger for technical support.

■ ABBREVIATIONS

LXR, Liver X receptor; LBD, ligand binding domain; DBD, DNA binding domain; HTS, high throughput screening; VS, virtual screening; WDI, world drug index; NCI, National Cancer Institute; EF, enrichment factor; HBA, hydrogen bond acceptor; HBD, hydrogen bond donor; HF, hydrophobic feature; AR, aromatic ring feature; HAF, hydrophobic aromatic feature; sh, shape; Xvols, exclusion volumes; SD standard deviation; RXR, retinoid X receptor

■ REFERENCES

(1) Auwerx, J.; Baulieu, E.; Beato, M.; Becker-Andre, M.; Burbach, P. H.; Camerino, G.; Chambon, P.; Cooney, A.; Dejean, A.; Dreyer, C.; Evans, R. M.; Gannon, F.; Giguere, V.; Gronemeyer, H.; Gustafson, J. A.; Laudet, V.; Lazar, M. A.; Mangelsdorf, D. J.; Milbrandt, J.; Milgrom, E.; Moore, D. D.; O'Malley, B.; Parker, M.; Parker, K.; Perlmann, T.; Pfahl, M.; Rosenfeld, M. G.; Samuels, H.; Schutz, G.; Sladek, F. M.; Stunnenberg, H. G.; Spedding, M.; Thummel, C.; Tsai, M. J.; Umesono, K.; Vennstrom, B.; Wahli, W.; Weinberger, C.; Willson, T. M.; Yamamoto, K. Nucl Receptors Nomenclature, C., A unified nomenclature system for the nuclear receptor superfamily. *Cell* **1999**, *97*, 161−163.

(2) Janowski, B. A.; Willy, P. J.; Devi, T. R.; Falck, J. R.; Mangelsdorf, D. J. An oxysterol signalling pathway mediated by the nuclear receptor LXR alpha. *Nature* **1996**, *383*, 728−731.

(3) Schultz, J. R.; Tu, H.; Luk, A.; Repa, J. J.; Medina, J. C.; Li, L. P.; Schwendner, S.; Wang, S.; Thoolen, M.; Mangelsdorf, D. J.; Lustig, K. D.; Shan, B. Role of LXRs in control of lipogenesis. *Genes Dev.* **2000**, *14*, 2831−2838.

(4) Bensinger, S. J.; Tontonoz, P. Integration of metabolism and inflammation by lipid-activated nuclear receptors. *Nature* **2008**, *454*, 470−477.

(5) Bensinger, S. J.; Bradley, M. N.; Joseph, S. B.; Zelcer, N.; Janssen, E. M.; Hausner, M. A.; Shih, R.; Parks, J. S.; Edwards, P. A.; Jamieson, B. D.; Tontonoz, P. LXR signaling couples sterol metabolism to proliferation in the acquired immune response. *Cell* **2008**, *134*, 97−111.

(6) Joseph, S. B.; Castrillo, A.; Laffitte, B. A.; Mangelsdorf, D. J.; Tontonoz, P. Reciprocal regulation of inflammation and lipid metabolism by liver X receptors. *Nat. Med.* **2003**, *9*, 213−219.

(7) Kalaany, N. Y.; Mangelsdorf, D. J. LXRs and FXR: The Yin and Yang of cholesterol and fat metabolism. *Annu. Rev. Physiol.* **2006**, *68*, 159−191.

(8) Collins, J. L.; Fivush, A. M.; Watson, M. A.; Galardi, C. M.; Lewis, M. C.; Moore, L. B.; Parks, D. J.; Wilson, J. G.; Tippin, T. K.; Binz, J. G.; Plunket, K. D.; Morgan, D. G.; Beaudet, E. J.; Whitney, K. D.; Kliewer, S. A.; Willson, T. M. Identification of a nonsteroidal liver X receptor agonist through parallel array synthesis of tertiary amines. *J. Med. Chem.* **2002**, *45*, 1963−1966.

(9) Bradley, M. N.; Hong, C.; Chen, M. Y.; Joseph, S. B.; Wilpitz, D. C.; Wang, X. P.; Lusis, A. J.; Collins, A.; Hseuh, W. A.; Collins, J. L.; Tangirala, R. K.; Tontonoz, P. Ligand activation of LXR beta reverses atherosclerosis and cellular cholesterol overload in mice lacking LXR alpha and apoE. *J. Clin. Investig.* **2007**, *117*, 2337−2346.

(10) Bennett, D. J.; Carswell, E. L.; Cooke, A. J.; Edwards, A. S.; Nimz, O. Design, structure activity relationships and X-ray co-crystallography of non-steroidal LXR agonists. *Curr. Med. Chem.* **2008**, *15*, 195−209.

(11) Goodwin, B. J.; Zuercher, W. J.; Collins, J. L. Recent advances in Liver X Receptor biology and chemistry. *Curr. Top. Med. Chem.* **2008**, *8*, 781−791.

(12) Hu, B.; Quinet, E.; Unwalla, R.; Collini, M.; Jetter, J.; Dooley, R.; Andraka, D.; Nogle, L.; Savio, D.; Halpern, A.; Goos-Nilsson, A.; Wilhelmsson, A.; Nambi, P.; Wrobel, J. Carboxylic acid based quinolines as liver X receptor modulators that have LXR beta receptor binding selectivity. *Bioorg. Med. Chem. Lett.* **2008**, *18*, 54−59.

(13) Hu, B.; Unwalla, R.; Collini, M.; Quinet, E.; Feingold, I.; Goos-Nilsson, A.; Wihelmsson, A.; Nambi, P.; Wrobel, J. Discovery and SAR of cinnolines/quinolines as liver X receptor (LXR) agonists with binding selectivity for LXR beta. *Biorg. Med. Chem.* **2009**, *17*, 3519−3527.

(14) Wrobel, J.; Steffan, R.; Bowen, S. M.; Magolda, R.; Matelan, E.; Unwalla, R.; Basso, M.; Clerin, V.; Gardell, S. J.; Nambi, P.; Quinet, E.; Reminick, J. I.; Vlasuk, G. P.; Wang, S.; Feingold, I.; Huselton, C.; Bonn, T.; Farnegardh, M.; Hansson, T.; Nilsson, A. G.; Wilhelmsson, A.; Zamaratski, E.; Evans, M. J. Indazole-based liver X receptor (LXR) modulators with maintained atherosclerotic lesion reduction activity but diminished stimulation of hepatic triglyceride synthesis. *J. Med. Chem.* **2008**, *51*, 7161−7168.

(15) Fievet, C.; Staels, B. Liver X receptor modulators: Effects on lipid metabolism and potential use in the treatment of atherosclerosis. *Biochem. Pharmacol.* **2009**, *77*, 1316−1327.

(16) Calkin, A. C.; Tontonoz, P. Liver X receptor signaling pathways and atherosclerosis. *Arterioscler. Thromb. Vasc. Biol.* **2010**, *30*, 1513−1518.

(17) Zuercher, W. J.; Buckholz, R. G.; Campobasso, N.; Collins, J. L.; Galardi, C. M.; Gampe, R. T.; Hyatt, S. M.; Merrihew, S. L.; Moore, J. T.; Oplinger, J. A.; Reid, P. R.; Spearing, P. K.; Stanley, T. B.; Stewart, E. L.; Willson, T. M. Discovery of tertiary sulfonamides as potent liver X receptor antagonists. *J. Med. Chem.* **2010**, *53*, 3412−3416.

(18) Joseph, S. B.; Bradley, M. N.; Castrillo, A.; Bruhn, K. W.; Mak, P. A.; Pei, L. M.; Hogenesch, J.; O'Connell, R. M.; Cheng, G. H.; Saez, E.; Miller, J. F.; Tontonoz, P. LXR-dependent gene expression is important for macrophage survival and the innate immune response. *Cell* **2004**, *119*, 299−309.

(19) Villablanca, E. J.; Raccosta, L.; Zhou, D.; Fontana, R.; Maggioni, D.; Negro, A.; Sanvito, F.; Ponzoni, M.; Valentinis, B.; Bregni, M.; Prinetti, A.; Steffensen, K. R.; Sonnino, S.; Gustafsson, J. A.; Doglioni, C.; Bordignon, C.; Traversari, C.; Russo, V. Tumor-mediated liver X receptor-alpha activation inhibits CC chemokine receptor-7 expression on dendritic cells and dampens antitumor responses. *Nat. Med.* **2010**, *16*, 98−105.

(20) Zelcer, N.; Khanlou, N.; Clare, R.; Jiang, Q.; Reed-Geaghan, E. G.; Landreth, G. E.; Vinters, H. V.; Tontonoz, P. Attenuation of neuroinflammation and Alzheimer's disease pathology by liver x receptors. *Proc. Natl. Acad. Sci. U.S.A.* **2007**, *104*, 10601−10606.

(21) Fitz, N. F.; Cronican, A.; Pham, T.; Fogg, A.; Fauq, A. H.; Chapman, R.; Lefterov, I.; Koldamova, R. Liver X receptor agonist treatment ameliorates amyloid pathology and memory deficits caused by high-fat diet in APP23 mice. *J. Neurosci.* **2010**, *30*, 6862−6872.

(22) Baranowski, M. Biological role of liver X receptors. *J. Physiol. Pharmacol.* **2008**, *59*, 31−55.

(23) Berman, H.; Westbrook, J.; Feng, Z.; Gilliland, G.; Bhat, T.; Weissig, H.; Shindyalov, I.; Bourne, P. The Protein Data Bank. *Nucleic Acids Res.* **2000**, *28*, 235−42.

(24) Berman, H.; Henrick, K.; Nakamura, H. Announcing the worldwide Protein Data Bank. *Nat. Struct. Mol. Biol.* **2003**, *10*, 980−980.

(25) Farnegardh, M.; Bonn, T.; Sun, S.; Ljunggren, J.; Ahola, H.; Wilhelmsson, A.; Gustafsson, J. A.; Carlquist, M. The three-dimensional structure of the liver X receptor beta reveals a flexible ligand-binding pocket that can accommodate fundamentally different ligands. *J. Biol. Chem.* **2003**, *278*, 38821−38828.

(26) Washburn, D. G.; Hoang, T. H.; Campobasso, N.; Smallwood, A.; Parks, D. J.; Webb, C. L.; Frank, K. A.; Nord, M.; Duraiswami, C.; Evans, C.; Jaye, M.; Thompson, S. K. Synthesis and SAR of potent LXR agonists containing an indole pharmacophore. *Bioorg. Med. Chem. Lett.* **2009**, *19*, 1097−1100.

(27) Chao, E. Y.; Caravella, J. A.; Watson, M. A.; Campobasso, N.; Ghisletti, S.; Billin, A. N.; Galardi, C.; Wang, P.; Laffitte, B. A.; Lannone, M. A.; Goodwin, B. J.; Nichols, J. A.; Parks, D. J.; Stewart, E.; Wiethe, R. W.; Williams, S. P.; Smallwood, A.; Pearce, K. H.; Glass, C.

K.; Willson, T. M.; Zuercher, W. J.; Collins, J. L. Structure-guided design of N-phenyl tertiary amines as transrepression-selective liver X receptor modulators with anti-inflammatory activity. *J. Med. Chem.* **2008**, *51*, 5758−5765.
(28) Jaye, M. C.; Krawiec, J. A.; Campobasso, N.; Smallwood, A.; Qiu, C. Y.; Lu, Q.; Kerrigan, J. J.; Alvaro, M. D. L.; Laffitte, B.; Liu, W. S.; Marino, J. P.; Meyer, C. R.; Nichols, J. A.; Parks, D. J.; Perez, P.; Sarov-Blat, L.; Seepersaud, S. D.; Steplewski, K. M.; Thompson, S. K.; Wang, P.; Watson, M. A.; Webb, C. L.; Haigh, D.; Caravella, J. A.; Macphee, C. H.; Willson, T. M.; Collins, J. L. Discovery of substituted maleimides as liver X receptor agonists and determination of a ligand-bound crystal structure. *J. Med. Chem.* **2005**, *48*, 5419−5422.
(29) Kher, S.; Lake, K.; Sircar, I.; Pannala, M.; Bakir, F.; Zapf, J.; Xu, K.; Zhang, S. H.; Liu, J. P.; Morera, L.; Sakurai, N.; Jack, R.; Cheng, J. F. 2-Aryl-N-acyl indole derivatives as liver X receptor (LXR) agonists. *Bioorg. Med. Chem. Lett.* **2007**, *17*, 4442−4446.
(30) Cheng, J. F.; Zapf, J.; Takedomi, K.; Fukushima, C.; Ogiku, T.; Zhang, S. H.; Yang, G.; Sakurai, N.; Barbosa, M.; Jack, R.; Xu, K. Combination of virtual screening and high throughput gene profiling for identification of novel liver X receptor modulators. *J. Med. Chem.* **2008**, *51*, 2057−2061.
(31) Ghemtio, L.; Devignes, M. D.; Smail-Tabbone, M.; Souchet, M.; Leroux, V.; Maigret, B. Comparison of three preprocessing filters efficiency in virtual screening: Identification of new putative LXR beta regulators as a test case. *J. Chem. Inf. Model.* **2010**, *50*, 701−715.
(32) Zhao, W.; Gu, Q.; Wang, L.; Ge, H.; Li, J.; Xu, J. Three-dimensional pharmacophore modeling of liver-X receptor agonists. *J. Chem. Inf. Model.* **2011**, *51*, 2147−2155.
(33) Beautrait, A.; Leroux, V.; Chavent, M.; Ghemtio, L.; Devignes, M. D.; Smaiel-Tabbone, M.; Cai, W.; Shao, X.; Moreau, G.; Bladon, P.; Yao, J.; Maigret, B. Multiple-step virtual screening using VSM-G: overview and validation of fast geometrical matching enrichment. *J. Mol. Model.* **2008**, *14*, 135−148.
(34) Leach, A. R.; Gillet, V. J.; Lewis, R. A.; Taylor, R. Three-dimensional pharmacophore methods in drug discovery. *J. Med. Chem.* **2010**, *53*, 539−558.
(35) Langer, T. Pharmacophores in drug research. *Mol. Inform.* **2010**, *29*, 470−475.
(36) Wolber, G.; Langer, T. LigandScout: 3-D pharmacophores derived from protein-bound Ligands and their use as virtual screening filters. *J. Chem. Inf. Model.* **2005**, *45*, 160−169.
(37) *OEChem*, version 1.7.0; OpenEye Scientific Software, I., Santa Fe, NM, USA; www.eyesopen.com, 2009.
(38) Grant, J. A.; Gallardo, M. A.; Pickup, B. T. A fast method of molecular shape comparison: A simple application of a Gaussian description of molecular shape. *J. Comput. Chem.* **1996**, *17*, 1653−1666.
(39) Williams, S.; Bledsoe, R. K.; Collins, J. L.; Boggs, S.; Lambert, M. H.; Miller, A. B.; Moore, J.; McKee, D. D.; Moore, L.; Nichols, J.; Parks, D.; Watson, M.; Wisely, B.; Willson, T. M. X-ray crystal structure of the liver X receptor beta ligand binding domain - Regulation by a histidine-tryptophan switch. *J. Biol. Chem.* **2003**, *278*, 27138−27143.
(40) Ratni, H.; Blum-Kaelin, D.; Dehmlow, H.; Hartman, P.; Jablonski, P.; Masciadri, R.; Maugeais, C.; Patiny-Adam, A.; Panday, N.; Wright, M. Discovery of tetrahydro-cyclopenta[*b*]indole as selective LXRs modulator. *Bioorg. Med. Chem. Lett.* **2009**, *19*, 1654−1657.
(41) Markt, P.; Petersen, R.; Flindt, E.; Kristiansen, K.; Kirchmair, J.; Spitzer, G.; Distinto, S.; Schuster, D.; Wolber, G.; Laggner, C.; Langer, T. Discovery of novel PPAR ligands by a virtual screening approach based on pharmacophore modeling, 3D shape, and electrostatic similarity screening. *J. Med. Chem.* **2008**, *51*, 6303−17.
(42) Noha, S. M.; Atanasov, A. G.; Schuster, D.; Markt, P.; Fakhrudin, N.; Heiss, E. H.; Schrammel, O.; Rollinger, J. M.; Stuppner, H.; Dirsch, V. M.; Wolber, G. Discovery of a novel IKK-beta inhibitor by ligand-based virtual screening techniques. *Bioorg. Med. Chem. Lett.* **2011**, *21*, 577−583.
(43) Fakhrudin, N.; Ladurner, A.; Atanasov, A. G.; Heiss, E. H.; Baumgartner, L.; Markt, P.; Schuster, D.; Ellmerer, E. P.; Wolber, G.; Rollinger, J. M.; Stuppner, H.; Dirsch, V. M. Computer-aided discovery, validation, and mechanistic characterization of novel neolignan activators of peroxisome proliferator-activated receptor gamma. *Mol. Pharmacol.* **2010**, *77*, 559−566.
(44) Waltenberger, B.; Wiechmann, K.; Bauer, J.; Markt, P.; Noha, S. M.; Wolber, G.; Rollinger, J. M.; Werz, O.; Schuster, D.; Stuppner, H. Pharmacophore modeling and virtual xcreening for novel acidic inhibitors of microsomal prostaglandin E-2 synthase-1 (mPGES-1). *J. Med. Chem.* **2011**, *54*, 3163−3174.
(45) Schuster, D.; Waltenberger, B.; Kirchmair, J.; Distinto, S.; Markt, P.; Stuppner, H.; Rollinger, J. M.; Wolber, G. Predicting cyclooxygenase inhibition by three-dimensional pharmacophoric profiling. Part I: model generation, validation and applicability in ethnopharmacology. *Mol. Inform.* **2010**, *29*, 75−86.
(46) Schuster, D. 3D pharmacophores as tools for activity profiling. *Drug Discovery Today: Technol.* **2010**, *7*, 205−211.
(47) Bernotas, R. C.; Singhaus, R. R.; Kaufman, D. H.; Travins, J. M.; Ullrich, J. W.; Unwalla, R.; Quinet, E.; Evans, M.; Nambi, P.; Olland, A.; Kauppi, B.; Wilhelmsson, A.; Goos-Nilsson, A.; Wrobel, J. 4-(3-Aryloxyaryl)quinoline sulfones are potent liver X receptor agonists. *Bioorg. Med. Chem. Lett.* **2010**, *20*, 209−212.
(48) Spencer, T. A.; Li, D. S.; Russel, J. S.; Collins, J. L.; Bledsoe, R. K.; Consler, T. G.; Moore, L. B.; Galardi, C. M.; McKee, D. D.; Moore, J. T.; Watson, M. A.; Parks, D. J.; Lambert, M. H.; Willson, T. M. Pharmacophore analysis of the nuclear oxysterol receptor LXR alpha. *J. Med. Chem.* **2001**, *44*, 886−897.
(49) Yang, C. D.; McDonald, J. G.; Patel, A.; Zhang, Y.; Umetani, M.; Xu, F.; Westover, E. J.; Covey, D. F.; Mangelsdorf, D. J.; Cohen, J. C.; Hobbs, H. H. Sterol intermediates from cholesterol biosynthetic pathway as liver X receptor ligands. *J. Biol. Chem.* **2006**, *281*, 27816−27826.
(50) Molteni, V.; Li, X.; Nabakka, J.; Liang, F.; Wityak, J.; Koder, A.; Vargas, L.; Romeo, R.; Mitro, N.; Mak, P. A.; Seidel, M.; Haslam, J. A.; Chow, D.; Tuntland, T.; Spalding, T. A.; Brock, A.; Bradley, M.; Castrillo, A.; Tontonoz, P.; Saez, E. N-acylthiadiazolines, a new class of liver x receptor agonists with selectivity for LXR beta. *J. Med. Chem.* **2007**, *50*, 4255−4259.
(51) Li, L. P.; Liu, J. W.; Zhu, L. S.; Cutler, S.; Hasegawa, H.; Shan, B.; Medina, J. C. Discovery and optimization of a novel series of liver X receptor-alpha agonists. *Bioorg. Med. Chem. Lett.* **2006**, *16*, 1638−1642.
(52) Liu, W. G.; Chen, S.; Dropinski, J.; Colwell, L.; Robins, M.; Szymonifka, M.; Hayes, N.; Sharma, N.; MacNaul, K.; Hernandez, M.; Burton, C.; Sparrow, C. P.; Menke, J. G.; Singh, S. B. Design, synthesis, and structure-activity relationship of podocarpic acid amides as Liver X receptor agonists for potential treatment of atherosclerosis. *Bioorg. Med. Chem. Lett.* **2005**, *15*, 4574−4578.
(53) Szewczyk, J. W.; Huang, S.; Chin, J.; Tian, J.; Mitnal, L.; Rosa, R. L.; Peterson, L.; Sparrow, C. P.; Adams, A. D. SAR studies: Designing potent and selective LXR agonists. *Bioorg. Med. Chem. Lett.* **2006**, *16*, 3055−3060.
(54) Panday, N.; Benz, J.; Blum-Kaelin, D.; Bourgeaux, V.; Dehmlow, H.; Hartman, P.; Kuhn, B.; Ratni, H.; Warot, X.; Wright, M. B. Synthesis and evaluation of anilinohexafluoroisopropanols as activators/modulators of LXR alpha and beta. *Bioorg. Med. Chem. Lett.* **2006**, *16*, 5231−5237.
(55) Hu, B. H.; Collini, M.; Unwalla, R.; Miller, C.; Singhaus, R.; Quinet, E.; Savio, D.; Halpern, A.; Basso, M.; Keith, J.; Clerin, V.; Chen, L.; Resmini, C.; Liu, Q. Y.; Feingold, I.; Huselton, C.; Azam, F.; Farnegardh, M.; Enroth, C.; Bonn, T.; Goos-Nilsson, A.; Wilhelmsson, A.; Nambi, P.; Wrobel, J. Discovery of phenyl acetic acid substituted quinolines as novel liver X receptor agonists for the treatment of atherosclerosis. *J. Med. Chem.* **2006**, *49*, 6151−6154.
(56) *Molecular Networks*; Molecular Networks: Erlangen, Germany.
(57) http://accelrys.com/products/discovery-studio/; Accelrys Software Inc.: San Diego, 2005.

(58) *Thompson Scientific*; Derwent Publications Ltd.: London, U.K., 2005.
(59) Milne, G. W. A.; Nicklaus, M. C.; Driscoll, J. S.; Wang, S. M.; Zaharevitz, D. National-Cancer-Institute drug information-system 3D Database. *J. Chem. Inf. Comput. Sci.* **1994**, *34*, 1219−1224.
(60) Güner, O. F.; Waldman, M.; Hoffmann, R.; Kim, J. H. *Strategies for Database Mining and Pharmacophore Development*; International University Line: La Jolla, CA, USA, 2000.
(61) Mills, J. E. J.; Dean, P. M. Three-dimensional hydrogen-bond geometry and probability information from a crystal survey. *J. Comput. Aided Mol. Des.* **1996**, *10*, 607−622.
(62) Schuster, D.; Markt, P.; Grienke, U.; Mihaly-Bison, J.; Binder, M.; Noha, S. M.; Rollinger, J. M.; Stuppner, H.; Bochkov, V. N.; Wolber, G. Pharmacophore-based discovery of FXR agonists. Part I: Model development and experimental validation. *Biorg. Med. Chem.* **2011**, *19*, 7168−7180.
(63) Hoerer, S.; Schmid, A.; Heckel, A.; Budzinski, R. M.; Nar, H. Crystal structure of the human liver X receptor beta ligand-binding domain in complex with a synthetic agonist. *J. Mol. Biol.* **2003**, *334*, 853−861.
(64) Svensson, S.; Ostberg, T.; Jacobsson, M.; Norstrom, C.; Stefansson, K.; Hallen, D.; Johansson, I. C.; Zachrisson, K.; Ogg, D.; Jendeberg, L. Crystal structure of the heterodimeric complex of LXR alpha and RXR beta ligand-binding domains in a fully agonistic conformation. *EMBO J.* **2003**, *22*, 4625−4633.